Diamond detectors for high energy physics experiments

Diamond detectors for high energy physics experiments

L. Bäni, A. Alexopoulos, M. Artuso, F. Bachmair, M. Bartosik, J. Beacham, H. Beck, V. Bellini, V. Belyaev, B. Bentele, et al.

Diamond detectors for high energy physics experiments

The RD42 collaboration

L. Bäni,[z,1] A. Alexopoulos,[c] M. Artuso,[v] F. Bachmair,[z] M. Bartosik,[c] J. Beacham,[o] H. Beck,[y] V. Bellini,[b] V. Belyaev,[n] B. Bentele,[u] E. Berdermann,[g] P. Bergonzo,[m] A. Bes,[ad] J-M. Brom,[i] M. Bruzzi,[e] M. Cerv,[c] G. Chiodini,[ac] D. Chren,[t] V. Cindro,[k] G. Claus,[i] J. Collot,[ad'] J. Cumalat,[u] A. Dabrowski,[c] R. D'Alessandro,[e] D. Dauvergne,[ad] W. de Boer,[l] C. Dorfer,[z] M. Dünser,[c] V. Eremin,[h] R. Eusebi,[aa] G. Forcolin,[x] J. Forneris,[q] H. Frais-Kölbl,[d] L. Gallin-Martel,[ad] M.L. Gallin-Martel,[ad] K.K. Gan,[o] M. Gastal,[c] C. Giroletti,[s] M. Goffe,[i] J. Goldstein,[s] A. Golubev,[j] A. Gorišek,[k] E. Grigoriev,[j] J. Grosse-Knetter,[y] A. Grummer,[w] B. Gui,[o] M. Guthoff,[c] I. Haughton,[x] B. Hiti,[k] D. Hits,[z] M. Hoeferkamp,[w] T. Hofmann,[c] J. Hosslet,[i] J-Y. Hostachy,[ad] F. Hügging,[a] C. Hutton,[s] H. Jansen,[c] J. Janssen,[a] H. Kagan,[o] K. Kanxheri,[ae] G. Kasieczka,[z] R. Kass,[o] F. Kassel,[l] M. Kis,[g] V. Konovalov,[o] G. Kramberger,[k] S. Kuleshov,[j] A. Lacoste,[ad] S. Lagomarsino,[e] A. Lo Giudice,[q] E. Lukosi,[ab] C. Maazouzi,[i] I. Mandic,[k] C. Mathieu,[i] M. Menichelli,[ae] M. Mikuž,[k] A. Morozzi,[ae] J. Moss,[o] R. Mountain,[v] S. Murphy,[x] M. Muškinja,[k] A. Oh,[x] P. Oliviero,[q] D. Passeri,[ae] H. Pernegger,[c] R. Perrino,[ac] F. Picollo,[q] M. Pomorski,[m] R. Potenza,[b] A. Quadt,[y] A. Re,[q] M. Reichmann,[z] G. Riley,[ab] S. Roe,[c] D. Sanz,[z] M. Scaringella,[e] D. Schaefer,[c] C.J. Schmidt,[g] S. Schnetzer,[p] S. Sciortino,[e] A. Scorzoni,[ae] S. Seidel,[w] L. Servoli,[ae] S. Smith,[o] B. Sopko,[t] V. Sopko,[t] S. Spagnolo,[ac] S. Spanier,[ab] K. Stenson,[u] R. Stone,[p] C. Sutera,[b] B. Tannenwald,[o] A. Taylor,[w] M. Traeger,[g] D. Tromson,[m] W. Trischuk,[r] C. Tuve,[b] L. Uplegger,[f] J. Velthuis,[s] N. Venturi,[r] E. Vittone,[q] S. Wagner,[u] R. Wallny,[z] J.C. Wang,[v] J. Weingarten,[y] C. Weiss,[c] T. Wengler,[c] N. Wermes,[a] M. Yamouni[ad] and M. Zavrtanik[k]

[a] *Universität Bonn, Bonn, Germany*
[b] *INFN/University of Catania, Catania, Italy*
[c] *CERN, Geneva, Switzerland*
[d] *FWT, Wiener Neustadt, Austria*
[e] *INFN/University of Florence, Florence, Italy*
[f] *FNAL, Batavia, U.S.A*
.[g] *GSI, Darmstadt, Germany*
[h] *Ioffe Institute, St. Petersburg, Russia*
[i] *IPHC, Strasbourg, France*
[j] *ITEP, Moscow, Russia*
[k] *Jožef Stefan Institute, Ljubljana, Slovenia* [l] *Universität Karlsruhe, Karlsruhe, Germany*
[m] *CEA-LIST Technologies Avancees, Saclay, France* [n] *MEPHI Institute, Moscow, Russia*
[o] *The Ohio State University, Columbus, OH, U.S.A.*
[p] *Rutgers University, Piscataway, NJ, U.S.A.*
[q] *University of Torino, Torino, Italy*
[r] *University of Toronto, Toronto, ON, Canada*
[s] *University of Bristol, Bristol, U.K.*
[t] *Czech Technical University, Prague, Czech Republic*
[u] *University of Colorado, Boulder, CO, U.S.A.*
[v] *Syracuse University, Syracuse, NY, U.S.A.*
[w] *University of New Mexico, Albuquerque, NM, U.S.A.*
[x] *University of Manchester, Manchester, U.K.*
[y] *Universität Göttingen, Göttingen, Germany*
[z] *ETH Zürich, Zürich, Switzerland*
[aa] *Texas A&M, College Park Station, TX, U.S.A.*

[ab]*University of Tennessee, Knoxville, TN, U.S.A.*
[ac]*INFN-Lecce, Lecce, Italy*
[ad]*LPSC-Grenoble, Grenoble, France*
[ae]*INFN-Perugia, Perugia, Italy*
[af] *California State University, Sacramento, CA, U.S.A.*

E-mail: lukas.baeni@phys.ethz.ch

Abstract

Beam test results of the radiation tolerance study of chemical vapour deposition (CVD) diamond against different particle species and energies is presented. We also present beam test results on the independence of signal size on incident particle rate in charged particle detectors based on unirradiated and irradiated poly-crystalline CVD diamond over a range of particle fluxes from 2 kHz/cm^2 to 10 MHz/cm^2. The pulse height of the sensors was measured with readout electronics with a peaking time of 6 ns. In addition functionality of poly-crystalline CVD diamond 3D devices was demonstrated in beam tests and 3D diamond detectors are shown to be a promising technology for applications in future high luminosity experiments.

Keywords

Diamond, Detectors; Particle tracking detectors; Radiation-hard detectors; Solid state detectors

1 Introduction

Diamond features some distinct properties which make it useful as a sensor material in applications with high fluences and/or high particle fluxes [1]. The large band gap (5.5 eV) of diamond allows operation at ambient temperature due to low leakage currents. Diamond's large displacement energy (42 eV) makes it inherently a radiation tolerant material. The RD42 collaboration has developed and studied position sensitive detectors based on chemical vapour deposition (CVD) diamond for the last 20 years [2–8]. As a result, diamond detectors have been successfully operating in beam monitoring systems of the present Large Hadron Collider (LHC) [9–13].

The innermost layers of tracking detectors and beam monitoring systems at the future High Luminosity LHC(HL-LHC) are expected to be exposed to a particle fluence of $\sim 2 \times 10^{16}$ hadrons cm^{-2} and a high particle rate of approximately 100 MHz cm^{-2} to 200 MHz cm^{-2} [14]. The RD42 collaboration studied the radiation tolerance of CVD diamond sensors against different particle species and energies as well as the signal response dependence on the particle rate up to a flux of 10 MHz cm^{-2}. Furthermore, devices with a 3D electrode geometry were developed and tested for applications at the HL-LHC. Results from these studies are presented in this paper.

2 Radiation tolerance

The RD42 collaboration has conducted a program to characterise the radiation tolerance of CVD diamond detectors. Multiple series of irradiations with protons and neutrons were carried out and their effect on the devices' signal response to charged particles was characterised.

One single-crystalline CVD (sCVD) diamond sample and three polycrystalline CVD (pCVD) diamond samples were irradiated with 800 MeV protons at the Los Alamos Neutron Science Center (LANSCE)

[15]. Two pCVD diamond samples were exposed to 70 MeV protons at the Cyclotron and Radioisotope Center of Tohoku University (CYRIC) [16] and a pCVD diamond sample was irradiated with fast reactor neutrons (> 100 keV) at the Jožef Stefan Institute (JSI) [17].

After each irradiation step, strip detectors were fabricated on the diamond samples. A 50 µm pitch strip detector was metallised on the growth side of the samples and a bias pad on the substrate side. Each strip was wire bonded to a VA2 readout channel [18] and the high voltage was applied on the bottom bias pad through an RC filter circuit.

The fully assembled detectors were probed in the H6 secondary beam line of the Super Proton Synchrotron (SPS) at CERN [19]. The beam line was tuned to a 120 GeV c^{-1} hadron beam. A high resolution beam telescope [20] consisting of four times two silicon strip planes was used to reconstruct tracks and predict the hit position in the diamond plane. A resolution on the predicted hit position of 1:3 µm was reached at the diamond plane. The readout was triggered using a 7 mm × 7 mm plastic scintillator. For each run, the first 10 % of the events were used to determine initial pedestals and for alignment. With the remaining events the device under test (DUT) was analysed. The signal response was measured as a function of the predicted hit position and the mean free path (MFP) was derived from the average pulse height.

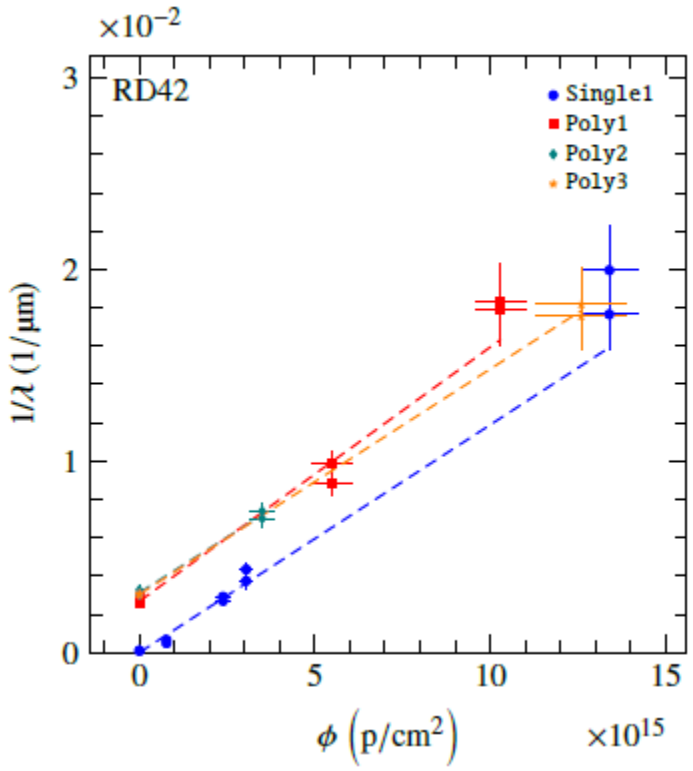

Figure 1. Inverse MFP as a function of 800 MeV proton fluence [21]. Error bars include statistical and systematic uncertainties added in quadrature. Reproduced with permission from [21]. @2018 ETH Library.

The MFP is inversely proportional to the trap density which increases linearly with fluence. Thus, the radiation damage model can be written as

$$\frac{1}{\lambda} = \frac{1}{\lambda_0} + k\,\emptyset \qquad (2.1)$$

where k is the *radiation damage constant*, $\emptyset$ is the fluence, and λ_0 is the initial MFP before irradiation. In figure 1, the inverse MFP is plotted as a function of 800 MeV proton fluence. An initial MFP of $10.0\ ^{+40}_{-6.5} \times 10^3$ µm was assumed for sCVD diamond, while the pCVD diamond samples' initial MFP was measured with a source setup and is smaller due to their higher initial trap density. The damage model was fitted to the data points of each sample. The parallel slopes indicate a common damage mechanism between sCVD and pCVD diamond.

Resulting slopes were averaged to derive the damage constant of 800 MeV protons. Damage constants for 70 MeV protons and fast neutrons were derived similarly. As a reference, the 24 GeV proton data from ref. [22] was re-evaluated by re-fitting using the above procedure. Table 1 summarises the relative damage constants.

Particle species	*k*
24 GeV protons	1
800 MeV protons	1.85 ± 0.13
70 MeV protons	2.5 ± 0.4
Fast neutrons	4.5 ± 0.5

Table 1. Relative radiation damage constants for different particle species [21]. Reproduced with permission from [21]. ©2018 ETH Library

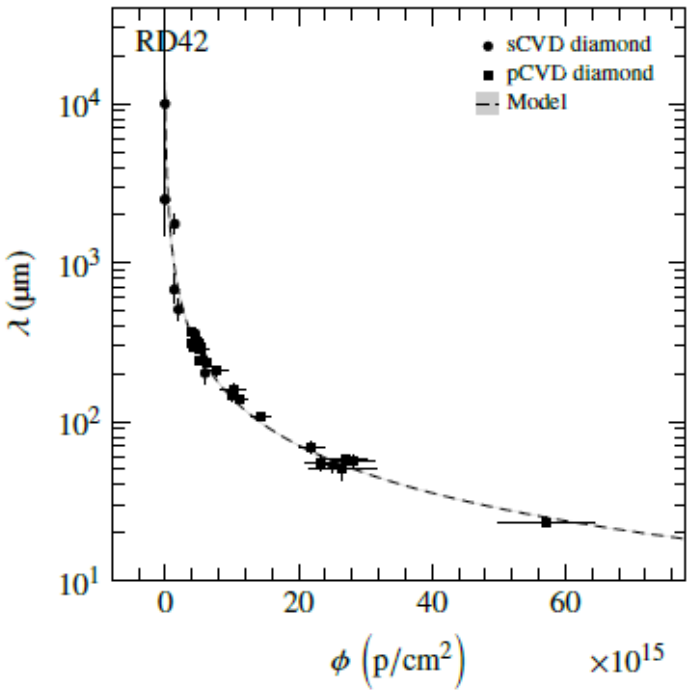

Figure 2. Mean free pass as a function of 24 GeV proton equivalent fluence [21]. Reproduced with permission from [21]. @2018 ETH Library.

In figure 2, the MFP is plotted as a function of 24 GeV proton equivalent fluence for all irradiated samples. In order to account for the number of traps in the initial state, an offset correction for the pCVD diamond samples of

$$\emptyset_0 = \frac{1}{k\ \lambda_0} \qquad (2.2)$$

was applied. The equivalent fluence was then derived by

$$\emptyset_{eq} = k\,\emptyset \qquad (2.3)$$

where k is the relative damage constant. With these corrections, the data in figure 2 line up clearly on a single damage curve.

3 Rate study

To measure the dependence of the signal response on the incident particle rate in diamond detectors, a series of beam tests [6, 23] was performed at the Paul Scherrer Institut (PSI) [24]. The M1 beam line of the High Intensity Proton Accelerator (HIPA) was tuned to a 260 MeV c^{-1} π^+ beam. The particle flux of this beam line can be varied from a rate of 5 kHz cm^{-2} to 20 MHz cm^{-2} with a bunch spacing of 19.8ns [25].

For this study the pCVD diamond samples were metallised with a pad configuration on both sides. A Cr/Au metallisation was used. The readout electronics were a modified version of a CERN fast amp [26] which has a peaking time of 6 ns and returns to baseline in 18 ns for a detector with a capacitance of 2 pF [23]. A beam telescope [27] made of silicon pixel detectors was used to track particles into the DUTs. The 100µm × 150µm pixel sensors were read out with the PSI46v2 readout chip [28]. The readout of the system was triggered by a scintillator and the amplified diamond signals were digitised with a DRS4 evaluation board [29]. A typical waveform of a diamond detector is shown in figure 3. The signal was measured at a fixed time of 69 ns after the trigger by taking the average in a 10 ns window around the peak.

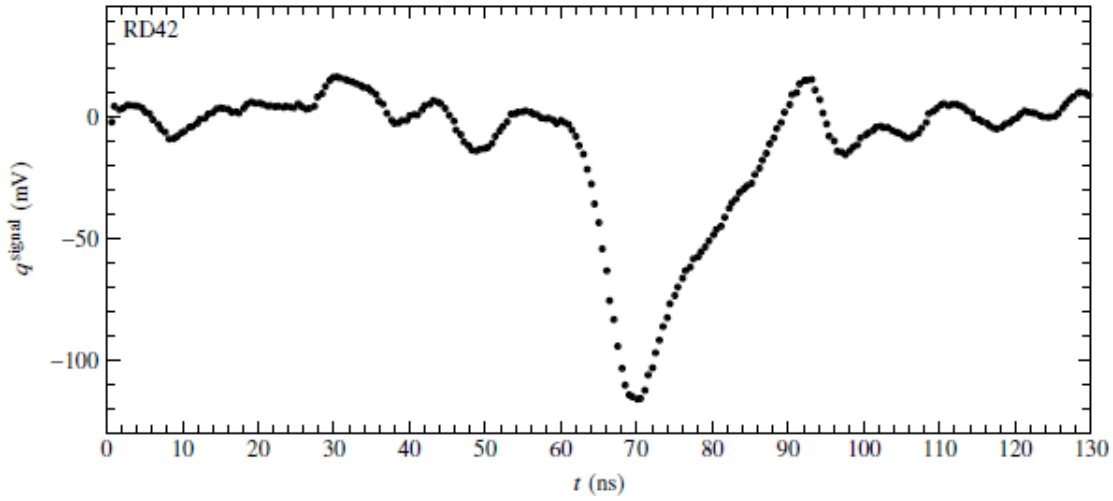

Figure 3. Sample signal trace of a diamond signal.

A measurement cycle included tests at different particle fluxes. After each test, the beam line was closed and tuned to the new particle flux. Tests up to a particle flux of 10 MHz cm^{-2} were performed. Figure 4 shows the pulse height, averaged over the entire detector, as a function of the particle flux for both positive and negative voltage. The signal response was observed to be independent of the particle flux up to a particle rate of 10 MHz cm^{-2}, both before and after a neutron fluence of 5×10^{14} n cm^{-2}. In this figure the pulse height units are arbitrary since the unirradiated and the irradiated detectors used different electronics. The resulting electronics gain corrections and the relative gain correction for different signal polarity in the electronics is still being determined and was not applied to the data in this figure.

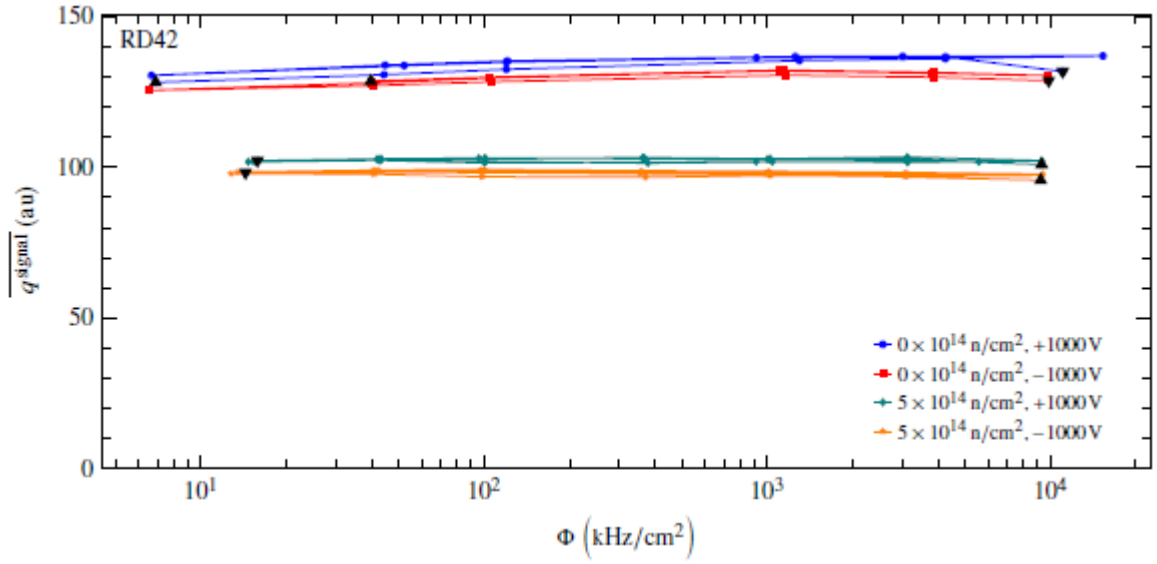

Figure 4. Average pulse height of pCVD diamond detectors as a function of particle flux before and after a neutron fluence of 5 × 10^{14} n cm^{-2} [23]. The black triangles indicate the start and end of a measurement cycle. Reproduced from [23]. Copyright owned by the original author(s) under the terms of the Creative Commons Attribution-NonCommercial-NoDerivatives 4.0 International License (CC BY-NC-ND 4.0)

4 3D diamond sensors

The concept of 3D detectors with electrodes in the bulk of the material was proposed in ref. [30]. Sensors with limited MFP, such as highly irradiated pCVD diamond or silicon detectors, may profit from the reduced charge carrier drift distance in 3D detectors.

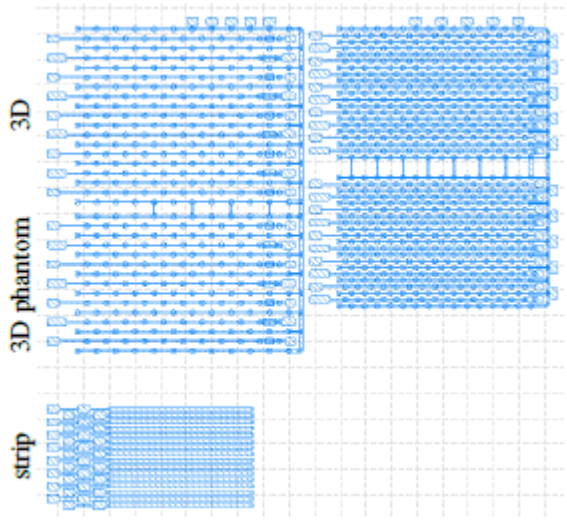

Figure 5. Metallisation mask [23]. The device is divided into three regions, each comprising a different detector: a 3D detector (top left) with a cell size of 150 µm × 150 µm, a 3D phantom detector (middle left) with the same metallisation pattern as the 3D detector but without any bulk electrodes, and a strip detector (bottom left) with a 50 µm strip pitch. The patterns on the right were not used. Reproduced from [23]. Copyright owned by the original author(s) under the terms of the

The RD42 collaboration successfully constructed a 3D detector based on sCVD diamond in 2015 [31]. Results of the first pCVD diamond 3D sensor are shown here and were published in 2016 [23]. The metallisation pattern of this device consists of three different regions as illustrated in figure 5. The first region is the 3D detector operated at a bias potential of 60 V. Its bulk column electrodes were fabricated with a laser as described in ref. [31]. These bulk column electrodes are connected to either readout or bias metal strips forming 99 150 µm × 150 µm cells. The second region is a 3D phantom detector with the same metallisation pattern as the previous region but without the bulk column electrodes. For reference, a 50 µm pitch strip detector defines the third pattern. The strip detector was operated at a bias voltage of 500 V.

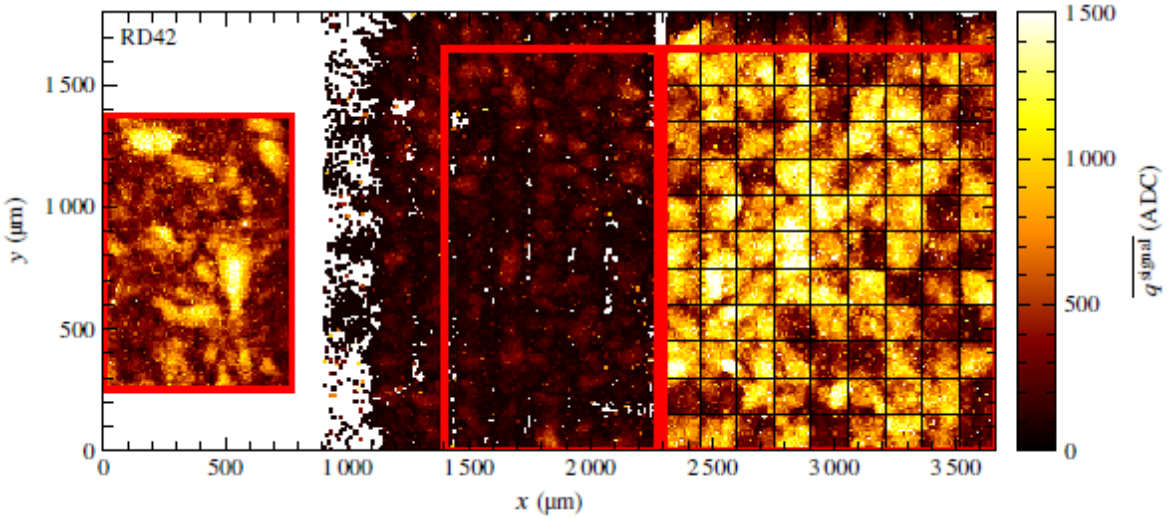

Figure 6. Average signal response as a function of predicted hit position in the diamond plane [23]. Reproduced from [23]. Copyright owned by the original author(s) under the terms of the Creative Commons Attribution-NonCommercial-NoDerivatives 4.0 International License (CC BY-NC-ND 4.0)

The multi-region device was probed with a beam telescope in a 120 $GeVc^{-1}$ hadron beam at CERN as described in section 2. Figure 6 shows the average pulse height of the multi-region device as a function of the predicted hit position. The 3D phantom region collects less charge than the other two regions. In the 3D region, some cells with decreased average pulse height due to broken readout columns were observed. In the further analysis, a contiguous fiducial region of working cells was defined. Figure 7 compares the signal response of this fiducial selection to the strip region. The average pulse height of the 3D region is roughly twice as large as the signal response of the strip detector and corresponds to 75% of full charge collection.

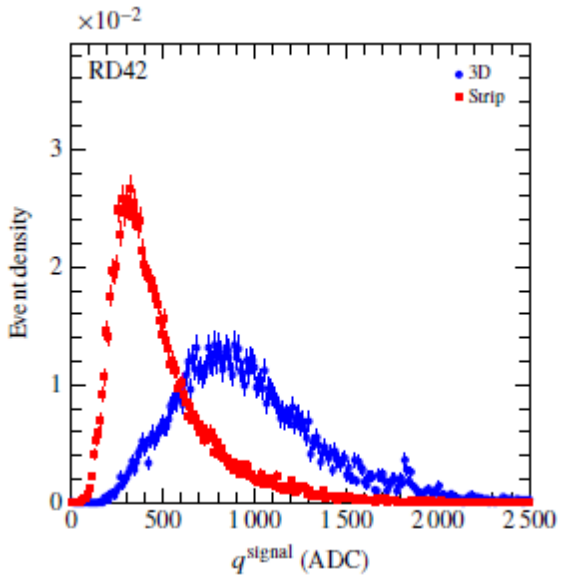

Figure7. Normalised pulse height distribution of the strip and 3D regions [23]. Reproduced from [23]. Copy-right owned by the original author(s) under the terms of the Creative Commons Attribution-NonCommercial-NoDerivatives 4.0 International License (CC BY-NC-ND 4.0)

In 2016, the RD42 collaboration assembled an improved full 3D device based on pCVD diamond. This device has a smaller cell size of 100 µm × 100 µm and with 1188 cells, an order of magnitude increase in number of cells. Furthermore, the column production efficiency was improved from 92 % to 99 %. Figure 8 shows the metallisation of the readout side with the 3D cells ganged together and read out as strips. With this full 3D device 85 % of the deposited charge was collected for the first time with a pCVD diamond device. The corresponding pulse height distribution is shown in figure 9.

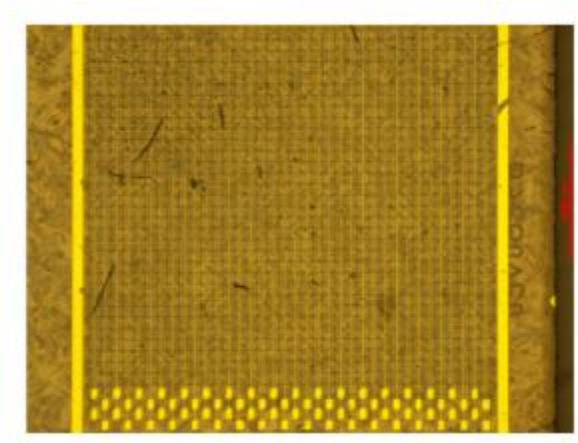

Figure 8. Photograph of the metallisation of the readout side. The bias column electrodes form a total of 1188 cells.

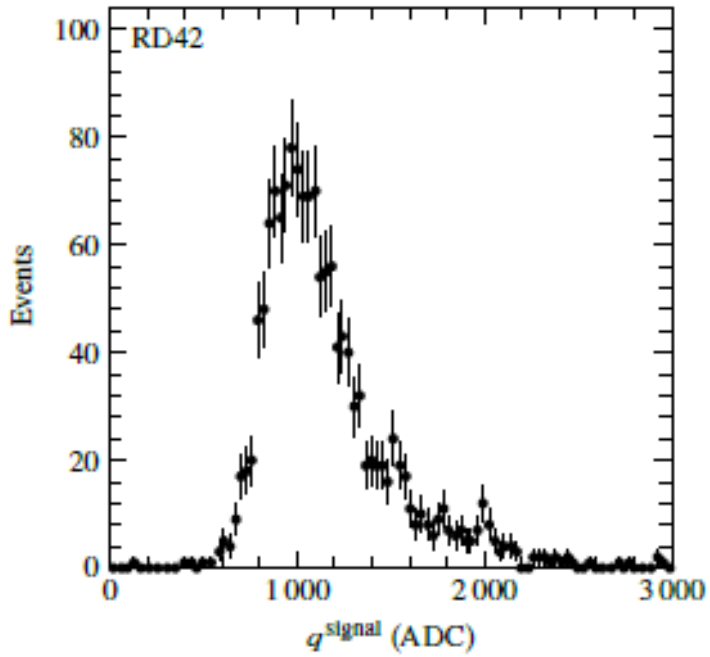

Figure 9. Pulse height distribution of the single 3D diamond device.

5 Conclusion

The radiation tolerance of CVD diamond sensors has been probed up to fluences relevant for tracking detectors at the HL-LHC. Before and after irradiation, the signal response of pCVD diamond detectors was observed to be independent of the particle rate up to a flux of 10 MHz cm^{-2}. The functionality of pCVD diamond 3D devices was demonstrated in beam tests. These results show 3D diamond detectors are a promising technology for applications in future HL-LHC experiments.

Acknowledgments

The RD42 collaboration gratefully acknowledges the staff at CERN for test beam time and their help in setting up beam conditions. We would especially like to thank Henric Wilkins, the test beam coordinator, for his assistance in making our tests a success. We would also like to thank the beam line staff at the PSI High Intensity Proton Accelerator. We would especially like to thank Konrad Deiters, Manuel Schwarz and Davide Reggiani of PSI for their assistance in carrying out the diamond detector tests. We also extend our gratitude to Prof. Lin Li and David Whitehead of the University of Manchester Laser Processing Center for assisting in the production of the 3D diamond device. The research leading to these results received funding from the European Union's Horizon 2020 research and innovation program under grant agreement No. 654168. This work was also partially supported by the Swiss National Science Foundation grant #20FL20_154216, ETH grant 51 15-1, Royal Society Grant UF120106 and U.S. Department of Energy grant DE-SC0010061.

References

[1] H. Kagan and W. Trischuk, *Radiation Sensors for High Energy Physics Experiments*, in *CVD Diamond for Electronic Devices and Sensors*, R.S. Sussmann eds., John Wiley, New York U.S.A. (2009).

[2] M.H. Nazaré et al., *Development of diamond tracking detectors for high luminosity experiments at the LHC*, R&D Proposal CERN/DRDC 94-21, DRDC/P56, CERN, Geneva Switzerland (1994).

[3] RD42 collaboration, F. Borchelt et al., *First measurements with a diamond microstrip detector*, *Nucl. Instrum. Meth.* **A 354** (1995) 318.

[4] RD42 collaboration, W. Adam et al., *The first bump-bonded pixel detectors on cvd diamond*, *Nucl. Instrum. Meth.* **A 436** (1999) 326–335.

[5] RD42 collaboration, W. Adam et al., *Radiation hard diamond sensors for future tracking applications*, *Nucl. Instrum. Meth.* **A 565** (2006) 278.